Coronal Seismology

Laurel Farris
New Mexico State University
laurel07@nmsu.edu

ABSTRACT

Coronal seismology involves the investigation of magnetohydrodynamic (MHD) waves and ocillatory phenomenae that arise in the solar corona. Here some of the dominant waves, oscillations, and modes are intimately investigated in the literature. Analysis of data from the Atmospheric Imaging Assembly (AIA) instrument on the Solar Dynamics Observatory (SDO) is also presented, both as stand-alone research and in the broader context of coronal seismology.

Subject headings: Sun: corona Sun: oscillations Sun: seismology

1. Introduction

The heating of the corona by magnetohydrodynamic (MHD) waves is one of two prevalent theories on how it reaches such high temperatures, the other being magnetic reconnection (Roberts et al. (1984)).

The basic types of MHD waves and oscillations are discussed in §2. §3 discusses each of the research topics in detail, including including references to work that has been done and is currently being carried out to address each one. §5 and §6 include a description of the research project and its implications for the broader field of coronal seismology. Conclusions and future work are summed up in §7.

2. Basic MHD

2.1. Types of Waves

In general, MHD waves are divided into two categories: Alfvén waves and magnetoacoustic waves. Magneto-acoustic waves can be further subdivided into slow-mode and fast-mode (Aschwanden (2004)). The slow-mode waves have phase speeds roughly equal to the sound speed in the medium in which they reside, analogous to typical acoustic waves, or sound waves. MHD studies usually focus on the fast-mode. Fast-mode magnetoacoustic waves have phase speeds comparable to the Alfvén speed, or $\omega/k \approx v_A$ (Aschwanden et al. (1999)). Two common fast modes in the corona are the asymmetric *kink* oscillations and symmetric *sausage* oscillations, which are discussed in more detail in §3.1 and §3.2, respectively.

The categories of MHD waves and oscillations can be best understood by their relative speeds. Figure 1 shows the wave speeds relative to the internal and external Alfvén and sound speeds.

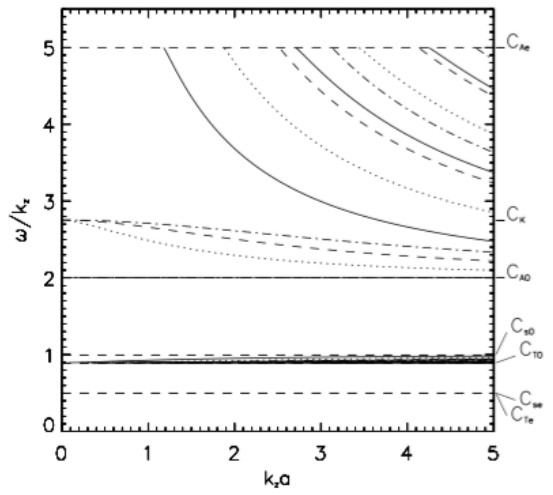

Fig. 1.— text (Image credit: Nakariakov & Verwichte (2005))

Each MHD mode is characterized based on a number of qualities, such as its wavelength, period, lifetime, speed, and whether it is propagting or standing, fast or slow, longitudinal or transverse, etc. The driving mechanisms that give rise to each mode can differ depending on these qualities and the environment in which the modes reside, and is one of the important MHD topics under investigation, along with the damping mechanism (Aschwanden et al. (1999)).

2.2. Equations and Models

MHD waves are often modeled with a cylindrical flux tube embedded in a magnetic field.

[cylindrical model, equations of ideal MHD, etc.]

$$\xi(x) = \xi(r)e^{i(kx+m\phi)} \tag{1}$$

For kink oscillations, m=1, and for sausage modes, m=0.

There are several equations for ideal MHD from which the dispersion relations are derived (I think).

2.3. Excitation and Damping Mechanisms

2.3.1. Resonant Absorption

2.3.2. Phase Mixing

2.4. Observation Techniques

Flux tubes (coronal loops), doppler shift and intensity variations, density variations, velocity and magnetic field values, etc. Coronal loops are density inhomogeneities in the corona, where the (low-β) plasma is "frozen-in" along the magnetic field lines whose feet are anchored in the photosphere.

3. Research Topics

3.1. Kink Oscillations

Kink oscillations are directly observed in coronal loops in extreme ultraviolet (EUV) wavelengths. They characterize the spacial oscillations that occur over the surface of the loop, perpendicular to the direction traversed by the length of the loop (Nakariakov & Verwichte (2005)). Kink oscillations generally are not accompanied by intensity variations; they displace the axis of the magnetic structure in which they propagate, but the cross-section of the waveguide remains roughly the same. Kink oscillations occur in the "long-wavelength regime", which is defined by the product of the wavenumber and the cross-section of the coronal loop being much less than 1 ($ka \ll 1$). In other words, the *wavelength* of the oscillation is much *greater* than the cross-section of the waveguide. The phase speed is just above the Alfvén speed within the loop, and the period of the oscillation is expected to be between $\sim$ 2 and 20 minutes (Aschwanden (2004)).

Due to a lack of sufficient instrumentation, spatial variations such as those caused by kink oscillations were not resolved until the launch of TRACE. Some of the first results from preliminary TRACE data were produced by Aschwanden et al. (1999) to investigate the oscillations present in coronal loops. Using 171 Å data, they modeled five loops that accompanied a class M4.6 solar flare in July of 1998. At this point, many MHD modes were characterized in theory

The observations had enough qualities characteristic of fast kink modes, including the spatial displacements characterisic of this asymmetrical mode, to identify these oscillations as kink modes. An average period of $T = 269 \pm 6$ seconds, or roughly 4.5 minutes, was obtained, which fit well with the theoretical period for kink oscillations. The absense of any phase shift along the length of the loops revealed that these were *standing waves*, with nodes located at the loop footpoints. The ability to identify kink modes has great significance for solar phsyics due to a correlation between the oscillation period and the magnetic field strength of the loop:

$$T \propto \frac{L}{\sqrt{n}}B \tag{2}$$

where T is the oscillation period, n is the number density, and B is the strength of the magnetic field.

More recently, Pascoe et al. (2015) investigated the driving mechanism behind the production, and damping of kink oscillations. They compared two possible functional form of the damping profile of the driver: that of a Gaussian and an exponential form. While the noise level of the data was too high to distinguish between the two forms, the simulations followed the form of a Gaussian.

They also considered the effect of the spatial profile of the driver itself on the excitation and subsequent damping of the kink waves. Two different possiblilities were explored here: the effect of a "highly structured" driver, which they found to be unrealistic, and the effects of eddies and photospheric motions around the footpoints of the coronal loops.

3.2. Sausage Oscillations

In contrast to kink oscillations, sausage oscillations do not displace the axis of the structure

in which they reside. However, they do cause a periodic change in the cross-section of the waveguide, and hence are observable through changes in intensity (and therefore density, due to flux conservation).

Lopin & Nagorny (2015) plotted the changes in intensity and cross-sectional area for sausage oscillations in photospheric pores extending up through the solar atmosphere. They used the general cylinder model for the pores, though it is more likely that the cross-sectional area of the waveguide increases with height as the temperature increases and density decreases. Sausage waves are characterized by a change in the cross-section, but no displacement of the loop axis. They occur on much shorter timescales than kink waves. The relationship between pore size and intensity can indicate

3.3. Acoustic Oscillations

The relatives periodicities of aacoustic oscillations were recognized as important characteristics, and modelled by Roberts et al. (1984). They recognized magnetoacoustic oscillations as a useful way to determine other properties of the solar atmosphere.

Srivastava & Dwivedi (2010) used intensity oscillations of a few different ionization species to pinpoint the orgin and progression of magnetoacoustic waves between bright points in the photosphere, through the transition regions, and up into the corona. The time series of intensity oscillations was converted into a power spectrum, and periodicities were extracted using wavelet analysis and periodograms (note here on what exactly these are?). The periods they derived ($\sim 263\pm80$ s for the He II 256.32 Å emission line and ($\sim 241\pm60$ s for the Fe XII 195.12 Å emission line) were close to the 5-minute global oscillations of the sun.

3.4. Propagating Acoustic Waves

While standing acoustic waves are primarily seen in closed coronal loops, propagating waves have been observed in both closed and open structures. The propagation speed of such waves is much lower than the local Alfvén speed, thus they are categorized as slow, longitudinal waves, (or magnetoacoustic waves), that travel along magnetic field lines at speeds roughly equal to the local sound speed. The changes in intensity along the same location as these waves propagate in time are mapped side by side to give time-distance information. The period, wavelength, propagation speed, and amplitude can all be derived using this method. Since the local sound, c_s is related to temperature, T, as

$$c_s \propto \sqrt{T} \tag{3}$$

a difference in observed propagation speeds implies a changing temperature profile in the transverse direction across the loop. (Nakariakov & Verwichte (2005)).

Propagating acoustic waves are generally observed as "propagating disturbances" awaiting further diagnoses of magnetoacoustic waves, whose amplitudes are rather weak, requiring careful, detailed data analysis to aquire good signal-to-noise (S/N).

One of the first studies to analyze simultaneous observations at different wavelengths was carried out by Robbrecht et al. (2001) using data from two different instruments: the Extreme ultraviolet Imaging Telescope (EIS) on the Solar and Heliospheric Observatory (SOHO) and the Transition Region And Coronal Explorer (TRACE). These wavelengths, along with their corresponding ions emitting at those wavelengths, the temperature, and other relevant quantities from the study are given in table 1. Both instruments observed AR

instrument	EIT	TRACE
ion	Fe XII	Fe IX
wavelength	195 Å	171 Å
cadence	15 s	25 s
temperature	1.6 MK	1 MK
sound speed	192 km s^{-1}	152 km s^{-1}
propagation speed	110 km s^{-1}	95 km s^{-1}

Table 1: Relevant quantities from Robbrecht et al. (2001)

8218, where the presence of "weak transient disturbances" were revealed, and later classified as slow, propagating magnetoacoustic waves, with speeds that varied between 65 and 150 km s^{-1}. The expression for the formal sound speed of the ambient region was given by

$$c_s = 152\ \sqrt{T}\ \text{m s}^{-1} \tag{4}$$

where T is in units of Kelvin. This was compared to the observed speed of the progating wave, which was derived from the slope of the "ridges" on each of the four time-distance plots. The propatation speed of each wave was slightly ($\sim$ same order of magnitude) lower than the local sound speed. This difference was due to the angle between the loop and the plane of the sky against which the observations were made. The amount of time for a disturbance to pass a particular point was determined to be ~ 169 s from the TRACE data. As both observations targeted the same wave, the signficance of the differing speeds for each observation indicated a temperature gradient in the loop itself, indicating either a bundle of loop threads that make up a single loop, or a number of concentric shells that make up a single loop.

A similar analysis in multiple wavelengths was carried out by Uritsky et al. (2013), using about 6 hours of observational data from the Atmospheric Imaging Assemply (AIA) on the Solar Dynamics Observatory (SDO). In addition to these observations, they introduced the "surfacing transform technique" in order to address the difficulty in extracting information from these low-amplitude waves amidst the noise (a typical signal-to-noise (S/N) ratio was ~ 0.1 %). (more information about this technique here?) This method involved the resonant behavior of "surfing signals", revealed during quasi-periodic disturbances.

This technique was applied to the lines at 131 Å, 171 Å, 193 Å, and 211 Å, over the active region (AR) NOAA AR 11082, where no sunspots were seen to be present and the flares were relatively low-energy. They found the same relationship between sound speed and temperature as shown in equation 3, though the driving mechanism for these disturbances was uncertain. The observed propagations were travelling primarily in the upward direction away from the footpoint, at speeds of about 40 to 180 km s^{-1} and periodicities between 4 and 8 minutes over all four channels.

3.5. Propagating Fast Waves

3.6. Torsional Modes

3.7. Mixed Modes

4. Discussion

The observational techniques and relevant properties of each of the different kinds of MHD waves are summarized in table 1.

5. Data

As part of the general topic of coronal seismology, a small research project was carried out as well, continuing over from several semesters previously. Several of the observational and analytical methods used in the literature were reproduced for this project.

6. Analysis

7. Conclusion

And we're finished.

REFERENCES

Aschwanden, M. 2004, Springer

Aschwanden, M. J., Fletcher, L., Schrijver, C. J., & Alexander, D. 1999, The Astrophysical Journal, 520, 880

Lopin, I., & Nagorny, I. 2015, ApJ, 810, 87

Nakariakov, V. M., & Verwichte, E. 2005, Living Rev. Solar Phys.

Pascoe, D. J., Wright, A. N., De Moortel, I., & Hood, A. W. 2015, A&A, 578, A99

Robbrecht, E., Verwichte, E., Berghmans, D., et al. 2001, A&A, 370, 591

Roberts, B., Edwin, P. M., & Benz, A. O. 1984, ApJ, 279, 857

Srivastava, A. K., & Dwivedi, B. N. 2010, MNRAS, 405, 2317

Uritsky, V. M., Davila, J. M., Viall, N. M., & Ofman, L. 2013, ApJ, 778, 26

This 2-column preprint was prepared with the AAS LaTeX macros v5.2.

Type of wave	Timescales	Sizescales	Observational techniques
Kink Oscillations	short	short	something
Sausage Oscillations	short	short	something
Acoustic Oscillations	x	x	x
Propagating	x	x	x